The non-contact detection and identification of blood stained fingerprints using visible wavelength hyperspectral imaging: part II effectiveness on a range of substrates

Abstract
Biological samples, such as blood, are regularly encountered at violent crime scenes and successful identification is critical for criminal investigations. Blood is one of the most commonly encountered fingerprint contaminants and current identification methods involve presumptive tests or wet chemical enhancement. These are destructive however; can affect subsequent DNA sampling; and do not confirm the presence of blood, meaning they are susceptible to false positives.
A novel application of visible wavelength reflectance hyperspectral imaging (HSI) has been used for the non-contact, non-destructive detection and identification of blood stained fingerprints across a range of coloured substrates of varying porosities. The identification of blood was based on the Soret γ band absorption of haemoglobin between 400 nm and 500 nm.
Ridge detail was successfully visualised to the third depletion across light coloured substrates and the stain detected to the tenth depletion on both porous and non-porous substrates. A higher resolution setup for blood stained fingerprints on black tiles, detected ridge detail to the third depletion and the stain to the tenth depletion, demonstrating considerable advancements from previous work. Diluted blood stains at 1500 and 1000 fold dilutions for wet and dry stains respectively were also detected on pig skin as a replica for human skin.

Keywords
Fingerprints, Blood detection, Forensic Science, Hyperspectral Imaging

Abbreviations
DS- Detect stain
DSLR- Digital single lens reflex
HSI- Hyperspectral imaging
PRD- Partial ridge detail
WRD- Whole ridge detail

Contents

1. Introduction 4
2. Material and Methods 5
2.1 Contamination of digit 5
2.2 HSI system- Version 1 5
2.3 HSI system- Version 2 5
2.4 Hyperspectral reflectance image acquisition and pre-processing 5
2.5 Criteria for the identification of blood stains 6
2.6 Grading of fingerprints 6
2.7 DSLR setup 6
2.8 Trials 7
2.8.1 Light/dark tiles 7
2.8.2 Black tiles with HSI setup version 2 7
2.8.3 Non-porous/porous substrates 7
2.8.4 Pig skin 7
3. Results and Discussion 8
3.1 Light/dark tiles 8
3.2 Black tiles with HSI setup version 2 9
3.3 Non-porous/porous substrates 9
3.4 Pig skin 10
4. Conclusion 11

1. Introduction

Various biological samples are regularly encountered at scenes of violent crime and the successful identification of these is of critical importance in criminal investigations. Of these biological samples, blood is one of the most commonly encountered [1] and is the most commonly observed fingerprint contaminant [2].

The successful identification of blood evidence depends on the ability to conclusively confirm the identity of an unknown substance as blood [3]. Existing wet chemical tests are presumptive only and will indicate on other non-blood substances, resulting in false positives [2]. An ideal method should be highly sensitive to blood and be effective even with blood diluted to latent levels in both stains and fingerprints. Additionally the method should be highly specific to avoid false positives.

One approach is to use non-contact non-destructive optical methods to analyse the sample and visible wavelength hyperspectral imaging has been previously reported for the detection of blood stains using the α and β bands between 500 nm and 600 nm [4-6]. This technique has been identified as a method for the rapid, non-destructive detection of blood stains in a presumptive manner. More recently our research group proposed a new blood stain identification approach using the Soret γ band absorption at 415 nm in haemoglobin for the confirmatory identification of blood [3]. This was shown to provide a higher sensitivity and specificity for the detection and identification of blood stains over previously proposed purely presumptive methods. Additional research by our group explored the effect of time on blood stains and a method for determining the age of blood stains was demonstrated [7,8]. This technique has so far only been applied to blood stains however, highlighting a novel application of visible wavelength hyperspectral imaging for the detection and identification of blood stained fingerprints. One of the key issues involving optical analysis of fingerprints is to ensure sufficient ridge detail is captured to allow for comparison of crime scene marks against fingerprints from a suspect.

The first part of this study [9] investigated the novel use of hyperspectral imaging for the analysis of blood stained fingerprints on white tiles. The main focus was to establish if ridge detail of a sufficient resolution could be determined, to potentially allow for fingerprint comparison. The outcome of this initial phase was that blood stained fingerprints to a significant number of depletions and dilutions were clearly identified, as well as ridge detail in blood stained fingerprints up to six months old. Blood stained fingerprints were also correctly identified against fingerprints contaminated with a range of red/brown contaminants, with zero false positives. A comparison of the effectiveness of HSI against the visualisation of ridge detail using DSLR photography also demonstrated significant advantages.

In this study we extend the novel application of this technique to the detection and identification of blood stained fingerprints across a range of different coloured substrates and porosities, which are representative of the types of substrates which may be encountered at crime scenes. Further comparison against the visualisation of ridge detail using DSLR photography on these substrates is discussed. Additional novel research is also presented exploring the analysis of blood stains on pig skin using hyperspectral analysis and preliminary findings are discussed following initial improvements to the hyperspectral prototype.

2. Material and Methods

2.1 Contamination of digit

Both human and horse blood were used as contaminants in this study. Human blood from a consenting healthy volunteer was used where the blood stains were to be analysed and disposed of within one day (trials 1-3). A sterile lancet (FinePoint, USA) in a Penlet Plus lancing device (LifeScan, USA) was used to pierce the left middle finger. The finger was gently squeezed to encourage blood flow and the resulting blood drops were evenly spread over the ridge detail on the right middle finger. In trial 4 screened horse blood was used. This was deposited into a Petri dish containing a small sponge. The right middle finger was pressed against the sponge to evenly coat the digit and the blood stained fingerprint was then deposited onto the substrate. Standard human and horse blood stained fingerprints were allowed to dry for approximately 1 hour before analysis. Wet samples were analysed within 20 minutes of deposition and dry samples were left to dry for 2 hours before analysis to ensure the entire deposited blood stain or fingerprint was dry. All substrates were cleaned with distilled water and thoroughly dried before labelling and fingerprint deposition. All pig skin (Danny's Butchers, Middlesbrough, UK) was flattened before deposition.

2.2 HSI system- Version 1

The HSI system (*Version 1*) used in this study was the same setup detailed in [3] and [9], consisting of a liquid crystal tuneable filter (LCTF) coupled to a 2.3 megapixel Point Grey camera and a light source for scene illumination. The light source was comprised of two 40W LEDs; one violet giving an output at 410nm and one white, giving an output between 450 and 700 nm. Control of the LCTF and image capture was performed using custom developed software written in C++ (Microsoft, USA). Images were captured between 400 nm and 680 nm with spectral sub sampling at 5 nm intervals, resulting in an image cube at 56 wavelengths for each scan. Spectra from the image cube were subsequently analysed using custom routines developed in Visual Studio (Microsoft, USA) and Spyder (Python, USA). The time required to acquire and process an image was approximately 30 seconds.

2.3 HSI system- Version 2

An improved version of the HSI system (*Version 2*) was create using an upgraded camera and an improved liquid crystal tuneable filter (LCTF). The camera was a 5.5 megapixel CMOS pco.edge camera coupled to a Varispec CRI liquid crystal tuneable filter. The same lighting setup was used as detailed above in **2.2**. Control of the LCTF and image capture was again performed using custom developed software written in C++ (Microsoft, USA), as detailed in **2.2**.

2.4 Hyperspectral reflectance image acquisition and pre-processing

The hyperspectral reflectance measurements were made following the method detailed in [3] and [9]. A reference image (R_0) was obtained using a blank ceramic tile. This image was recorded in a 5 nm series of 56 discrete wavelengths between 400 nm and 680 nm. The sample image (R_s) was recorded at the same wavelengths under the same illumination conditions and integration time settings on the camera. The hyperspectral reflectance image (R) consisted of a data cube of 1280 × 1024 pixel values at 56 discrete wavelengths. Additional information regarding sample image processing can be found in [3].

2.5 Criteria for the identification of blood stains

The presence of haemoglobin in blood dominates the blood reflectance spectrum in the visible region [7,8]. The spectrum contains a strong narrow absorption at 415 nm called the Soret or γ band with two weaker and broader absorptions between 500 and 600 nm known as the β and α bands [3]. Due to the absorption in the blue part of the visible spectrum, the Soret band is responsible for giving blood its distinctive red colour. Other red substances also absorb in the blue region of the visible spectrum between 400 and 680 nm. However, the width of these absorption features is typically much broader and also not centred at 415 nm. This forms the basis of the methodology to identify and discriminate blood stains from other similarly coloured substances. Further information is detailed in [3]. From the reflectance images obtained, the pixels which satisfied the criterion were marked as black, whilst all other pixels were marked as white. This allowed regions of the image where the blood stained fingerprint was present to be identified, as well as clear distinction of the ridge detail.

2.6 Grading of fingerprints

The same grading method was used as detailed in Part 1 [9] and the trials involving 6 or 12 print depletion series were assessed based on three factors- the furthest deposition where it was possible to detect second level ridge detail (eg. bifurcations, ridge endings) across the whole of fingerprint (whole ridge detail, WRD), where it was possible to detect some second level ridge detail (partial ridge detail, PRD), and where it was possible to detect the blood stain but no ridge detail at any level could be resolved (detect stain, DS). Whole ridge detail was assigned a score of three, partial ridge detail a score of two, detecting the stain a score of one, and no visualisation a score of zero as shown in ***Figure 1***.

This grading method was used by the same experienced investigator for all fingerprints to compare the sensitivity of the techniques. The further down the depletion series ridge detail could be detected across the whole fingerprint, the higher the sensitivity of the technique. A single individual was used to grade all fingerprints, so as to remove the additional variable of subjective grading from different individuals. Fingerprints were graded from the on screen images generated by the custom software following hyperspectral analysis and the DSLR images copied from the memory card.

[Insert Figure 1]

Figure 1: Grading scale used for comparing the visualisation of second level ridge detail in blood stained fingerprints and the overall fingerprint stain between techniques, with example hyperspectral images for each grading score

2.7 DSLR setup

The images used in this report were taken using a digital single lens reflex (DSLR) camera mounted on a Kaiser RS1 copy stand. The DSLR was a Canon EOS 700D which was fitted with a Canon Angle Finder C 90° viewfinder with a 1.25-2.5x optical magnification and a Canon TC-80N3 remote control external shutter release to avoid camera motion. Images were taken using two sizes of macro lenses- a 50mm lens for overview shots of the substrates and a 100mm lens for high magnification macro shots of individual fingerprints. The 50mm lens was used as it is recognised as being generally equivalent to the view seen by the human eye [10]. The lenses used were a Canon EF 50mm f2.5 macro lens and a Canon EF 100mm f2.8L macro IS USM lens. Substrates were lit using oblique lighting from two Daylight Twist Portable Lamps with a white light output of 6500K. Images were captured in aperture priority mode with an aperture of f/8 to ensure clarity of focus across the whole fingerprint and an

ISO between 100 and 400 to minimise noise or grain in the images. The lighting setup in combination with the selected DSLR camera settings were determined in preliminary studies where clear second level ridge detail could be observed. DSLR images were saved onto a SanDisk 16GB memory card and transferred to a PC for grading.

2.8 Trials

Four trials were designed to explore fingerprint detection and realisation of ridge detail using both HSI setup *Version 1* and *Version 2* in comparison to ridge detail visible by DSLR. All fingerprints were deposited by one male donor (age 26, omnivore, no cosmetics).

2.8.1 Light/dark tiles

Depletion series of 12 fingerprints in undiluted human blood were deposited onto twelve ceramic tiles, categorised as light/dark in ***Table 1***. White and black were included in the light and dark categorisations respectively. Each tile was photographed and then analysed using HSI *Version 1*.

[Insert Table 1]

Table 1: Twelve different coloured ceramic tiles and their light/dark classification on which blood stained fingerprints were deposited for comparison between DSLR photography and HSI Version 1

2.8.2 Black tiles with HSI setup version 2

Due to the issues surrounding the detection of blood on dark substrates, further research exploring black tiles was carried out. Depletion series of 12 fingerprints in undiluted human blood were deposited onto black tiles. Each tile was photographed and then analysed using HSI *Version 2*.

2.8.3 Non-porous/porous substrates

Depletion series of 12 fingerprints in undiluted human blood were deposited onto thirteen substrates of varying porosity; six non-porous and seven porous substrates, as detailed in ***Table 2***. Each substrate was photographed and then analysed using HSI *Version 1*.

[Insert Table 2]

Table 2: Thirteen substrates divided into porous and non-porous categories on which blood stained fingerprints were deposited for comparison between DSLR photography and HSI Version 1

2.8.4 Pig skin

Preliminary experiments identified pig skin as a suitable substitute for human skin. The sensitivity of HSI to detect diluted blood stains on pig skin was explored using horse blood diluted with distilled water (10 fold to 5000 fold). 12 dilutions, as shown in ***Table 3***, were deposited (10 μL) onto two pieces of pig skin. Each piece was photographed and then one was analysed with wet stains within 20 minutes. The other piece was left to dry for 2 hours prior to analysis, as detailed in **2.1**. Analysis of both pieces of pig skin was carried out using HSI setup *Version 1*.

[Insert Table 3]

Table 3: Concentrations of diluted blood stains used to determine the sensitivity of HSI setup Version 1 compared to DSLR photography on pig skin

3. Results and Discussion

The volume of human blood used was less than analyses involving horse blood, although comparisons are only reported between the same contaminant, where similar volumes were used (human with human, horse with horse).

3.1 Light/dark tiles

Analysis of the 12 depletions using HSI *Version 1* detected whole and partial ridge detail across the full range of coloured substrates explored. A comparison of the DSLR and hyperspectral images on the coloured tiles is shown for the first depletion in ***Figure 2***.

On average, ridge detail was detected to the 3rd depletion across all light tiles with HSI and the stain detected to the 12th, as shown in ***Figure 3***. The HSI results are comparable with the success of visualisation using DLSR for the first few depletions but are better from the 8th depletion onwards. Although no ridge detail is observable, on average HSI detected the stain to the 12th depletion compared to the 7th with DSLR. This demonstrates a considerable benefit of using HSI over DSLR, as not only is the sensitivity greater across a range of light coloured tiles, but the detection confirms the presence of blood in the deposited fingerprint.

On average, ridge detail was detected to the 2nd depletion across all dark tiles with HSI and the stain detected to the 7th, as shown in ***Figure 4***. The visualisation of blood stained fingerprints using HSI *Version 1* on dark coloured tiles is not as good as DSLR photography, predominantly due to the success of oblique lighting allowing for the visualisation of the latent fingerprint after the loss of the blood contaminant with DSLR. However HSI has the advantage of being able to confirm the presence of blood.

As expected the HSI results on light tiles were better than on dark tiles, as shown in ***Figure 5***.This is because dark substrates absorb too much of the incident light resulting in a noisy reflectance image. This issue has been addressed and an improved setup with a more sensitive scientific grade camera has been used to explore black tiles, as discussed in **3.2**. A greater difference was present between the initial depositions on light and dark tiles than the lower depletions, which indicates that the colour of the substrate affects the ability of HSI to detect ridge detail more significantly than detection of the stain alone. This difference between light and dark substrates was considerably smaller at lower depletions with reduced ridge detail.

[Insert Figure 2]

Figure 2: Images of 1st depletion on light (left) and dark (right) coloured tiles: DSLR (top) and HSI Version 1 (below)

[Insert Figure 3]

Figure 3: A comparison of the mean scores for DSLR and HSI for 12 depletions across light coloured substrates

[Insert Figure 4]

Figure 4: A comparison of the mean scores for DSLR and HSI for 12 depletions across dark coloured substrates

[Insert Figure 5]

Figure 5: A comparison of the mean HSI scores for 12 depletions across light and dark coloured substrates

3.2 Black tiles with HSI setup version 2

Initial results with HSI *Version 2* demonstrated significantly improved sensitivity to blood stained fingerprints on black tiles, as whole and partial ridge detail were detected to the 2nd and 3rd depletions respectively. The stain was still detected to the 10th depletion on black tiles, although ridge detail was no longer observable **Error! Reference source not found.**. The same fingerprint viewed by DSLR showed partial ridge detail visible to the 11th depletion, although it was the white latent fingerprint ridge detail in contrast to the dark substrate visible rather than the blood stained fingerprint. Further development of this improved HSI setup is required to ensure HSI is comparable to DSLR photography, even with oblique lighting allowing for the visualisation of the latent fingerprint with DSLR after the loss of the blood contaminant. Further improvements to the custom software are required to allow for hyperspectral images generated to be exported for comparison.

3.3 Non-porous/porous substrates

Analysis of the 12 depletions using HSI detected whole and partial ridge detail across all non-porous and porous substrates explored, apart from red and black cotton. Due to the open nature of the weave and the porous nature of the substrate, no ridge detail was observed on red or black cotton with either HSI or DSLR, as the blood diffused rapidly into the fabric. A comparison of the DSLR and hyperspectral images is shown for the first depletion on non-porous and porous substrates in ***Figure 6***.

On average, ridge detail was detected to the 4th depletion across all non-porous substrates with HSI and the stain detected to the 10th, as shown in ***Figure 7***. The HSI results are comparable with the success of visualisation using DLSR for the first few depletions but are slightly better from the 6th depletion onwards. Although no ridge detail is observable, on average HSI detected the stain to the 10th depletion compared to the 7th with DSLR. This demonstrates a considerable benefit of using HSI over DSLR, as not only is the sensitivity greater across the range of non-porous substrates explored, but the detection confirms the presence of blood in the deposited fingerprint.

Ridge detail was detected for the 1st depletion across all porous substrates (apart from red and black cotton) with HSI and the stain detected to the 10th, as shown in ***Figure 8***. The visualisation of blood stained fingerprints using HSI *Version 1* on porous substrates is comparable to DSLR photography across all depositions, predominantly due to the reduced visualisation of ridge detail generally due to the porous substrates rapidly absorbing the deposited blood stained fingerprints. However HSI has the advantage of being able to confirm the presence of blood, and could even still detect the stain to the 10th depletion on average, despite the absorbent nature of the substrates.

As expected the average scores obtained from HSI analysis on non-porous substrates were higher than on porous substrates, as shown in ***Figure 9***. This is because of the diffusion and absorption of the blood contaminant reduced the quality of the ridge detail observable, particularly on the cotton fabrics.

A greater difference was present between the initial depositions on non-porous and porous substrates than the lower depletions, which indicates, as expected, that the substrate porosity affects the ability of HSI to detect ridge detail more significantly than detection of the stain

alone. This difference between non-porous and porous substrates was considerably smaller from the 9th depletion, due to the general lower levels of ridge detail present.

[Insert Figure 6]

Figure 6: Images of 1st depletion on non-porous (left) and porous (right) substrates: DSLR (top) and old setup HSI images (below)

[Insert Figure 7]

Figure 7: A comparison of the mean scores for DSLR and HSI for 12 depletions across non-porous substrates

[Insert Figure 8]

Figure 8: A comparison of the mean scores for DSLR and HSI for 12 depletions across porous substrates

[Insert Figure 9]

Figure 9: A comparison of the mean HSI scores for 12 depletions across non-porous and porous substrates

3.4 Pig skin

Using HSI *Version 1*, wet stains were detected to 1500 fold dilutions, as shown in ***Figure 10***. Dry stains were only detected to 1000 fold dilutions on pig skin, as there was considerable noise within the image. This is expected however, as the increased time since deposition for dry stains allows for decomposition processes to take place, potentially reducing the concentration of haemoglobin slightly within the deposited stain. A 1500 fold dilution corresponds to 0.067% of the deposited material composed of blood. Each stain was composed of 10 μL of diluted blood, which equates to around 6.7 nL of blood at 1500 fold dilutions for wet stains and 10 nL of blood at 1000 fold dilutions for dry stains on pig skin. However, this limit could be improved by increasing the exposure time, as that would increase the amount of light entering the camera and possibly improve the signal-to-noise ratio. This could be particularly beneficial for the examination of skin on both suspects or victims, as it could allow for the detection and identification of blood stains, even after the blood has been sufficiently diluted to result in latent blood stains not easily observable during a visual examination with the naked eye.

[Insert Figure 10]

Figure 10: Images of wet (top) and dry (below) diluted stains on pig skin: DSLR (left) and HSI (right)

4. Conclusion

A novel implementation of visible wavelength reflectance hyperspectral imaging has been used for the non-contact and non-destructive detection and positive identification of blood stained fingerprints on a range of substrates of differing colour and porosity. In the processed hyperspectral images, pixels where blood was identified were coloured black whilst all other pixels were coloured white, thus enhancing the location of ridge detail in blood stained fingerprints. This is the first time HSI has been used to visualise fingerprints in blood across a wide range of substrates with both wet and dry stains and demonstrates a potential considerable advantage over existing chemical enhancement methods, as HSI analysis is both non-contact and non-destructive, thereby minimising any damage to the ridge detail present. This also could remove the need for presumptive tests, which could destroy part of a sample and reduce the volume of material available for further forensic tests, such as DNA analysis.

Additionally hyperspectral analysis is considerably quicker than the current workflow for the identification of blood involving presumptive tests followed by confirmatory techniques, such as DNA analysis. Using HSI, a blood stained fingerprint can be analysed and the blood positively identified within thirty seconds. This could be particularly beneficial for cases which require a rapid turnaround of forensic results in order to charge a suspect within the 24 hour PACE window or where there is considerable suspected blood evidence at a scene. Due to the non-destructive nature of HSI, analysis could also be beneficial for substrates where conventional enhancement techniques may not be possible, such as with particularly delicate substrates or locations where chemical methods might be unsafe.

Further work is required to compare the effectiveness of HSI for the detection of blood stained fingerprints against existing chemical enhancement methods, so as to explore the potential of implementing HSI within the existing forensic workflow for blood detection and identification. A comparison of the effectiveness of HSI both before and after chemical enhancement could demonstrate an additional potential application of the method as a non-contact rapid confirmatory technique following standard presumptive tests. The images currently generated by the existing hyperspectral setup are not of sufficient resolution to allow for real-world comparison between fingerprints and crime scene marks, but planned improvements to the prototype should increase this resolution sufficiently. Improvements to the custom software should also allow for images from the HSI Version 2 setup to be more effectively compared. Development of a more rugged instrument could lead on to a robust portable device which could be used at crime scenes. Previous research exploring the age determination of blood stains could also be applied to blood stained fingerprints, which would allow for both the non-contact, non-destructive identification and visualisation of ridge detail and a determination of the age of the blood with which the fingerprint was deposited.

References

[1] Jonathan Finnis, Jennie Lewis, Andrew Davidson, Comparison of methods for visualizing blood on dark surfaces, *Science & Justice*, 53, 2, (2013), 178-186
[2] Home Office CAST, Fingerprint Sourcebook, Chapter 3, 3.1 Acid Dyes, 1st ed., Home Office, 2013
[3] Bo Li, Peter Beveridge, William T. O'Hare, Meez Islam, The application of visible wavelength reflectance hyperspectral imaging for the detection and identification of blood stains, *Science & Justice,* 54, 6, (2014), 432-438
[4] Suwatwong Janchaysang, Sarun Sumriddetchkajorn, Prathan Buranasiri, Tunable filter-based multispectral imaging for detection of blood stains on construction material substrates Part 2: realization of rapid blood stain detection, *Applied Optics,* 52, 20, (2013), 4898-4910
[5] Suwatwong Janchaysang, Sarun Sumriddetchkajorn, Prathan Buranasiri, Tunable filter-based multispectral imaging for detection of blood stains on construction material substrates Part 1: Developing blood stain discrimination criteria, *Applied Optics,* 51, 29, (2012), 6984-6996
[6] G. J. Edelman, E. Gaston, T. G. van Leeuwen, P. J. Cullen, M. C. G. Aalders, Hyperspectral imaging for non-contact analysis of forensic traces, *Forensic science international,* 223, 1–3, (2012), 28-39
[7] Bo Li, Peter Beveridge, William T. O'Hare, Meez Islam, The age estimation of blood stains up to 30 days old using visible wavelength hyperspectral image analysis and linear discriminant analysis, *Science & Justice,* 53, 3, (2013), 270-277
[8] Bo Li, Peter Beveridge, William T. O'Hare, Meez Islam, The estimation of the age of a blood stain using reflectance spectroscopy with a microspectrophotometer, spectral pre-processing and linear discriminant analysis, *Forensic science international,* 212, 1–3, (2011), 198-204
[9] Samuel Cadd, Bo Li, Peter Beveridge, William T. O'Hare, Andy Campbell, Meez Islam, Non-contact detection and identification of blood stained fingerprints using visible wavelength reflectance hyperspectral imaging: part 1, *Science and Justice,* (2016)
[10] Michael Langford, Anna Fox, Richard Sawdon Smith, Langford's Basic Photography, 8th ed., Focal Press, Oxford, 2009

Table 1

Colour	Light/Dark
White	Light
Yellow	Light
Light Blue	Light
Green	Light
Grey	Light
Red	Dark
Blood Red	Dark
Dark red	Dark
Blue	Dark
Brown	Dark
Black	Dark

Table 2

POROUS/NON-POROUS	SUBSTRATE	COLOUR/INFO
NON-POROUS	GLASS	-
	PLASTIC BAGS	TESCO (OLD) [PLAIN]
		TESCO (OLD) [PATTERNED]
		TESCO (NEW)
		BIN BAGS (WHITE)
		BIN BAGS (BLACK)
POROUS	PAPER	-
	COTTON	WHITE
		RED
		BLACK
	CARDBOARD	BROWN
	WOOD	WHITE MELAMINE COATED CHIPBOARD
		PINE

Table 3

Summary of Dilutions			
Number	**Ratio**	**X fold**	**% Concentration**
1	1:0	Pure	100.000%
2	1:9	10 fold	10.000%
3	1:49	50 fold	2.000%
4	1:99	100 fold	1.000%
5	1:199	200 fold	0.500%
6	1:499	500 fold	0.200%
7	1:999	1000 fold	0.100%
8	1:1499	1500 fold	0.067%
9	1:1999	2000 fold	0.050%
10	1:2999	3000 fold	0.033%
11	1:3999	4000 fold	0.025%
12	1:4999	5000 fold	0.020%

Figure 1

Observable second level ridge detail	Abbreviation	Grading Score	HSI Example Image
Whole ridge detail	WRD	3	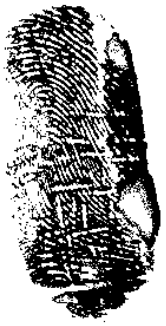
Partial ridge detail	PRD	2	
Detect stain only	DS	1	
No stain visible	-	0	

Figure 2

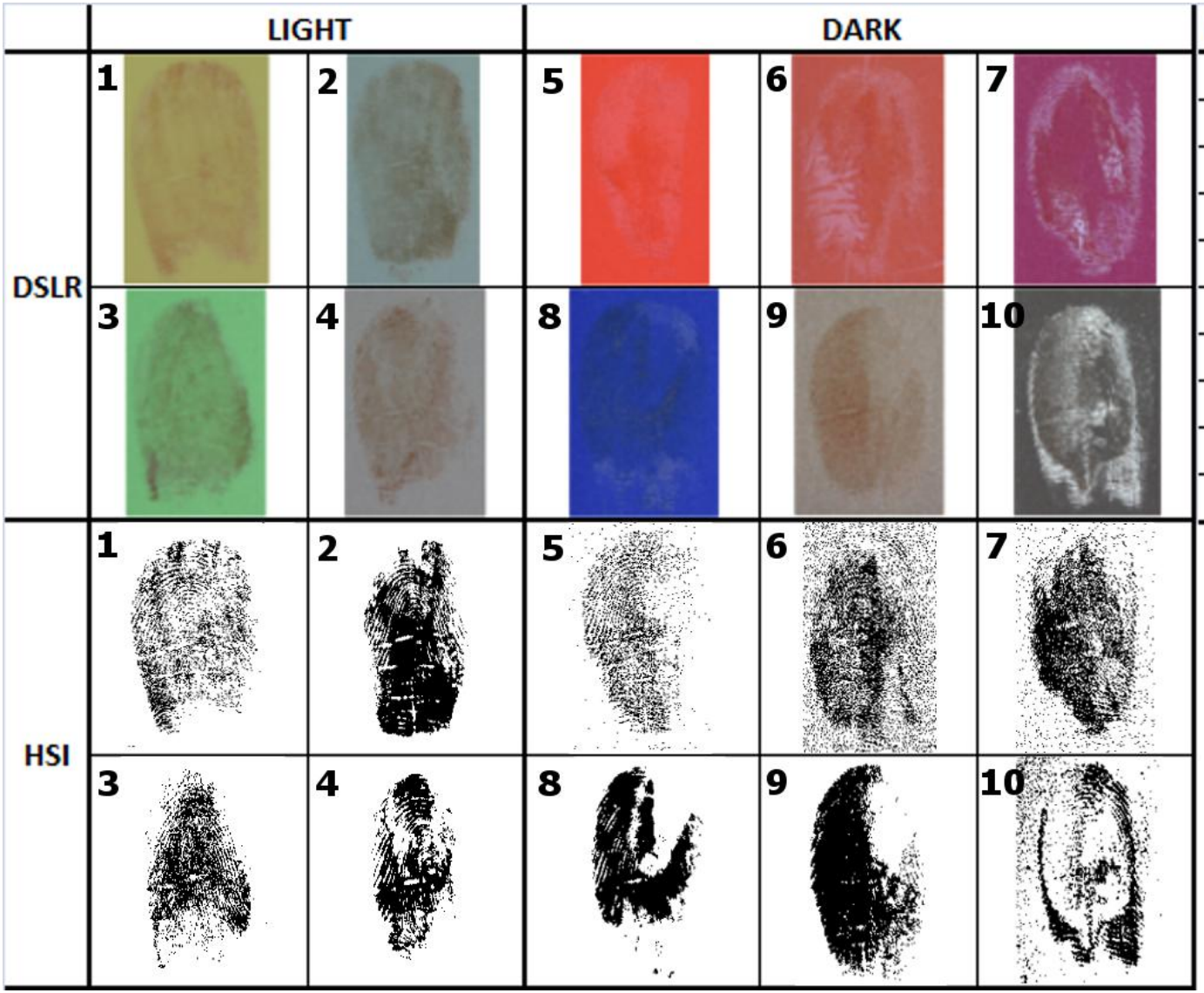

NUMBER	COLOUR
1	Yellow
2	Light Blue
3	Green
4	Grey
5	Red
6	Blood Red
7	Dark red
8	Blue
9	Brown
10	Black

Figure 3

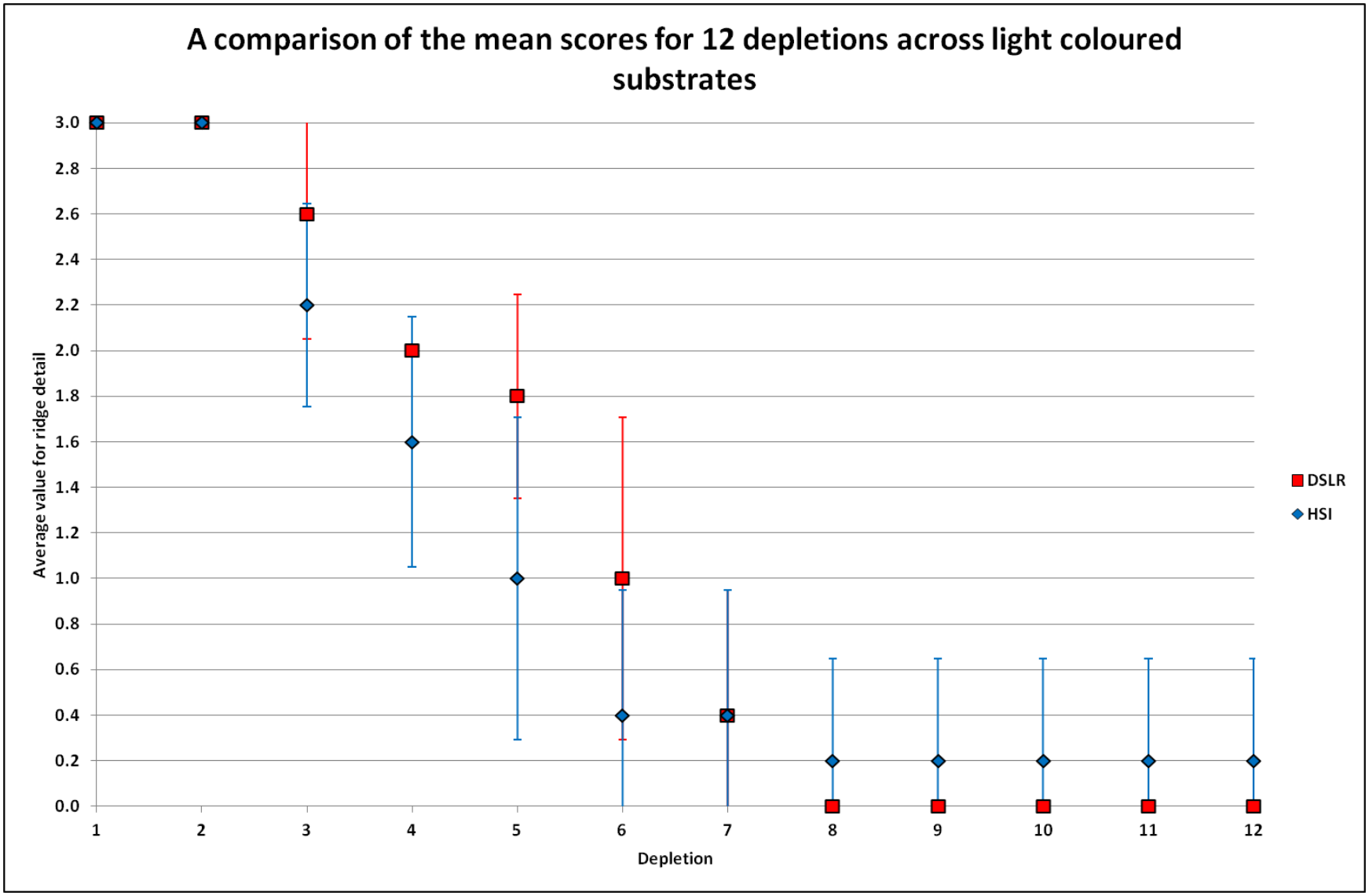
A comparison of the mean scores for 12 depletions across light coloured substrates
Average value for ridge detail
3.0
2.8
2.6
2.4
2.2
2.0
1.8
1.6
1.4
1.2
1.0
0.8
0.6
0.4
0.2
0.0
1
2
3
4
5
6
7
8
9
10
11
12
Depletion
DSLR
HSI

Figure 4

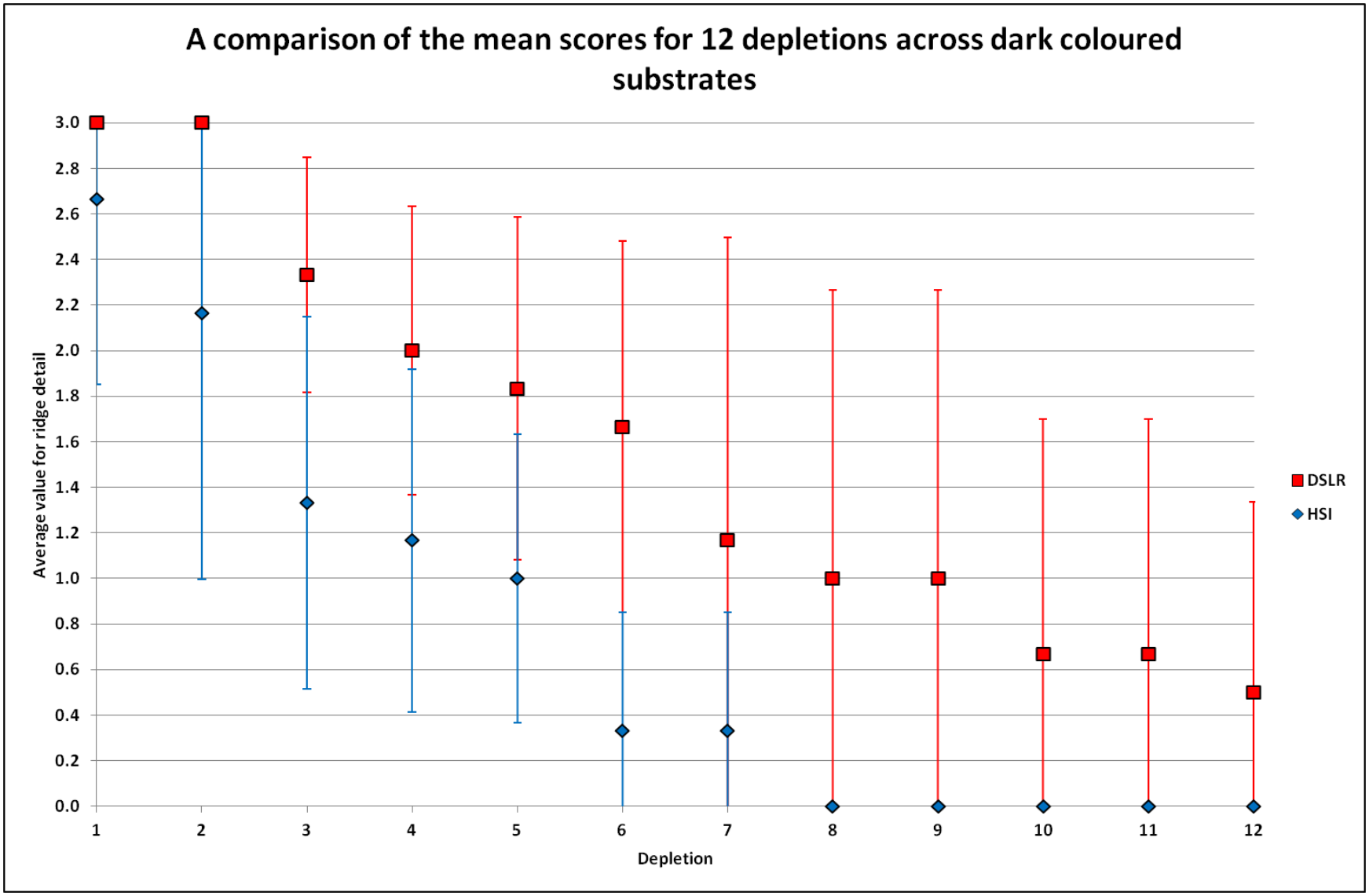
A comparison of the mean scores for 12 depletions across dark coloured substrates
Average value for ridge detail
3.0
2.8
2.6
2.4
2.2
2.0
1.8
1.6
1.4
1.2
1.0
0.8
0.6
0.4
0.2
0.0
1
2
3
4
5
6
7
8
9
10
11
12
Depletion
DSLR
HSI

Figure 5

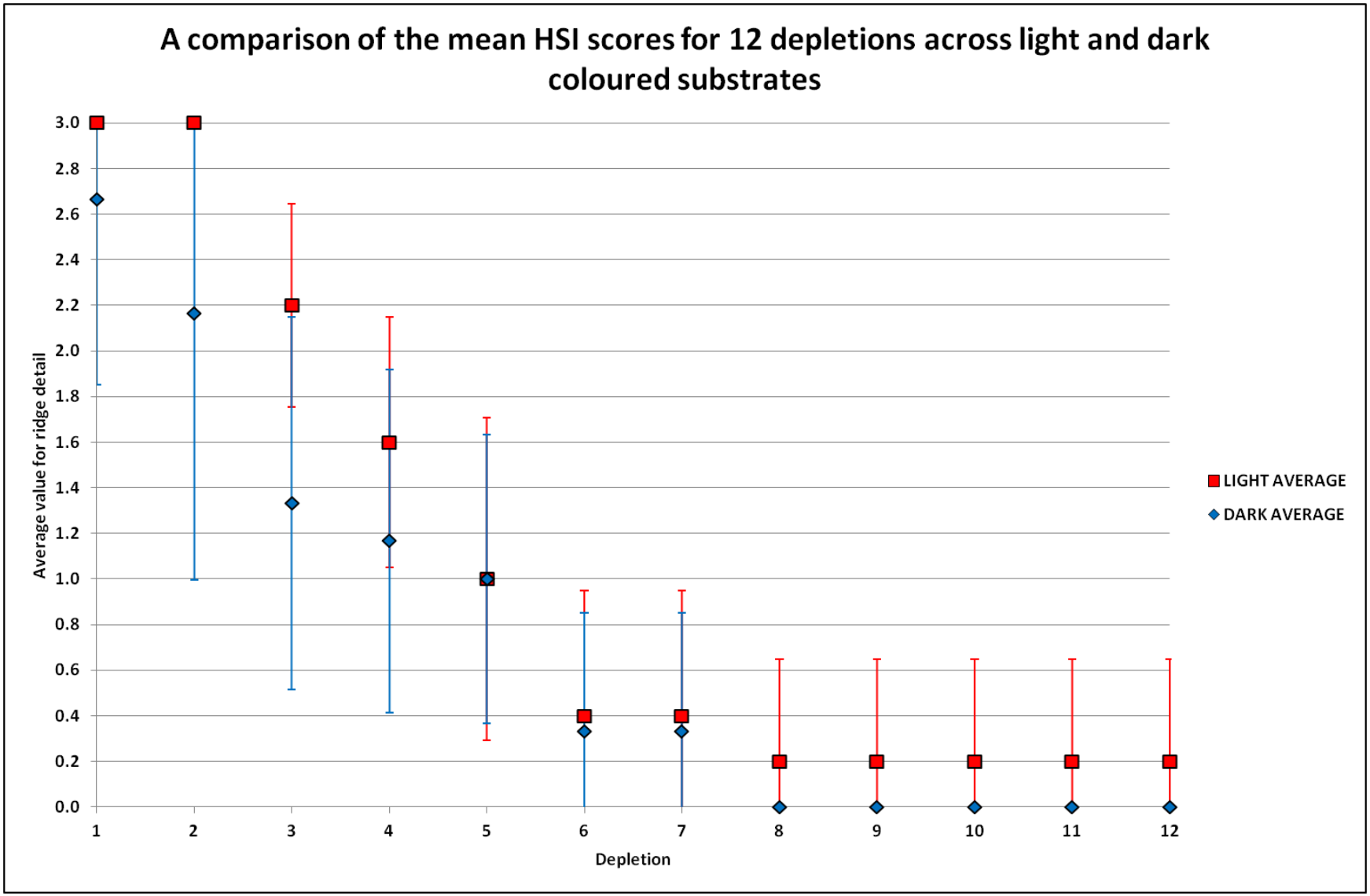
A comparison of the mean HSI scores for 12 depletions across light and dark coloured substrates
Average value for ridge detail
3.0
2.8
2.6
2.4
2.2
2.0
1.8
1.6
1.4
1.2
1.0
0.8
0.6
0.4
0.2
0.0
1
2
3
4
5
6
7
8
9
10
11
12
Depletion
LIGHT AVERAGE
DARK AVERAGE

Figure 6

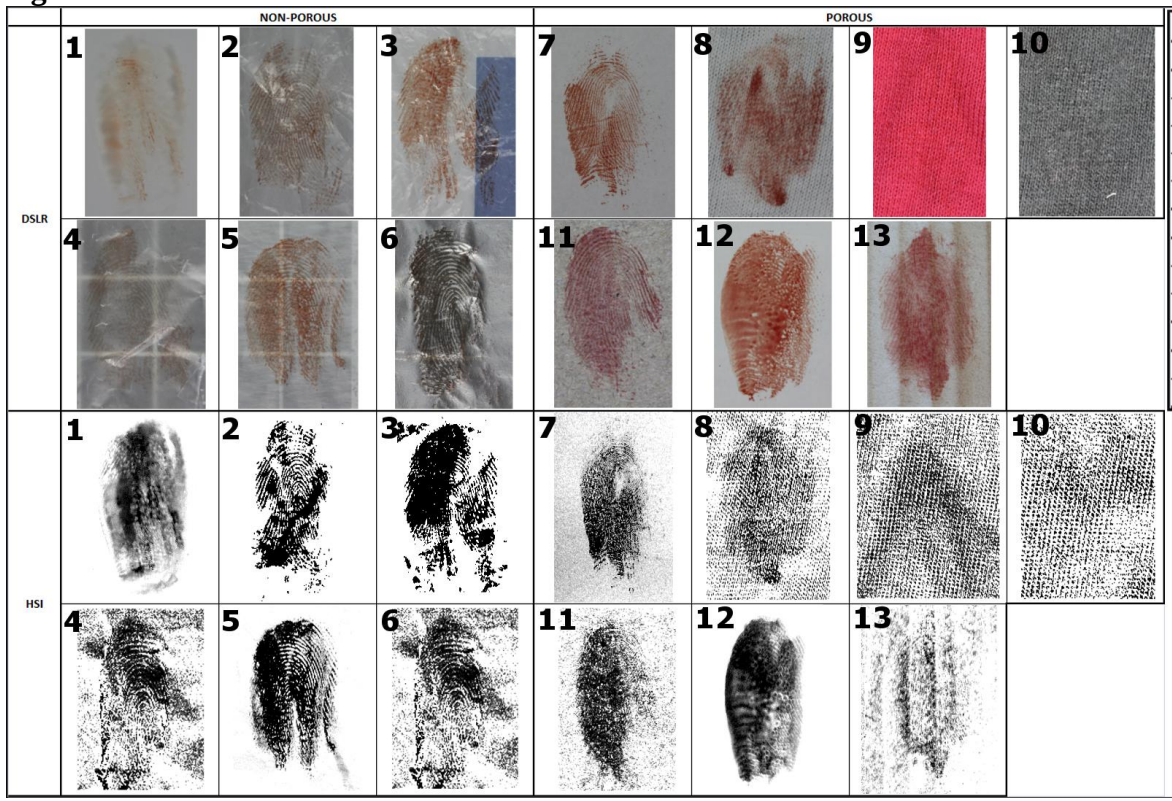

NUMBER	SUBSTRATE	COLOUR/INFO
1	GLASS	-
2	PLASTIC BAGS	TESCO (OLD) [PLAIN]
3		TESCO (OLD) [PATTERNED]
4		TESCO (NEW)
5		BIN BAGS (WHITE)
6		BIN BAGS (BLACK)
7	PAPER	-
8	COTTON	WHITE
9		RED
10		BLACK
11	CARDBOARD	BROWN
12	WOOD	WHITE MELAMINE COATED CHIPBOARD
13		PINE

Figure 7

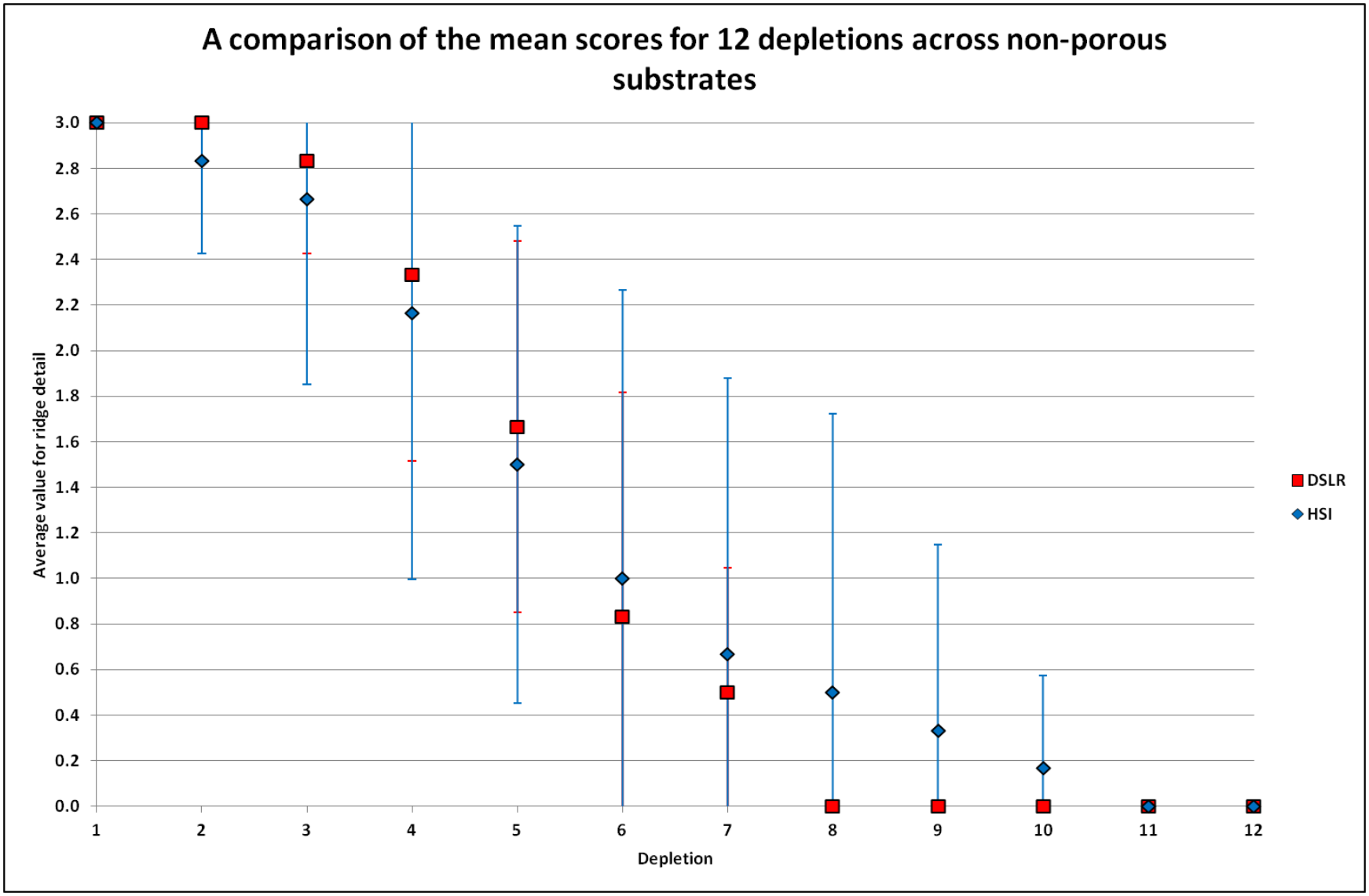
A comparison of the mean scores for 12 depletions across non-porous substrates
Average value for ridge detail
3.0
2.8
2.6
2.4
2.2
2.0
1.8
1.6
1.4
1.2
1.0
0.8
0.6
0.4
0.2
0.0
1
2
3
4
5
6
7
8
9
10
11
12
Depletion
DSLR
HSI

Figure 8

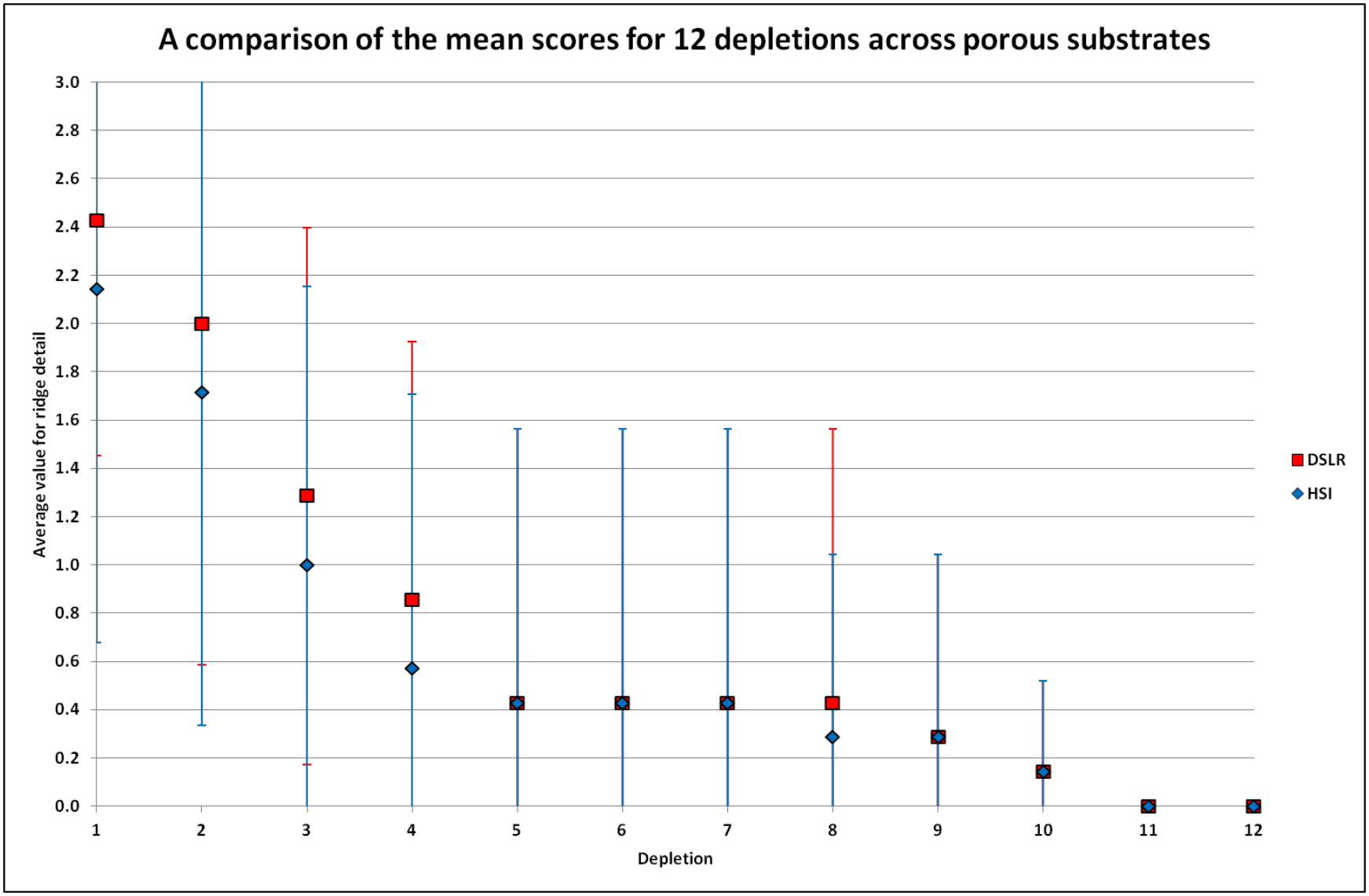
A comparison of the mean scores for 12 depletions across porous substrates
Average value for ridge detail
3.0
2.8
2.6
2.4
2.2
2.0
1.8
1.6
1.4
1.2
1.0
0.8
0.6
0.4
0.2
0.0
1
2
3
4
5
6
7
8
9
10
11
12
Depletion
DSLR
HSI

Figure 9

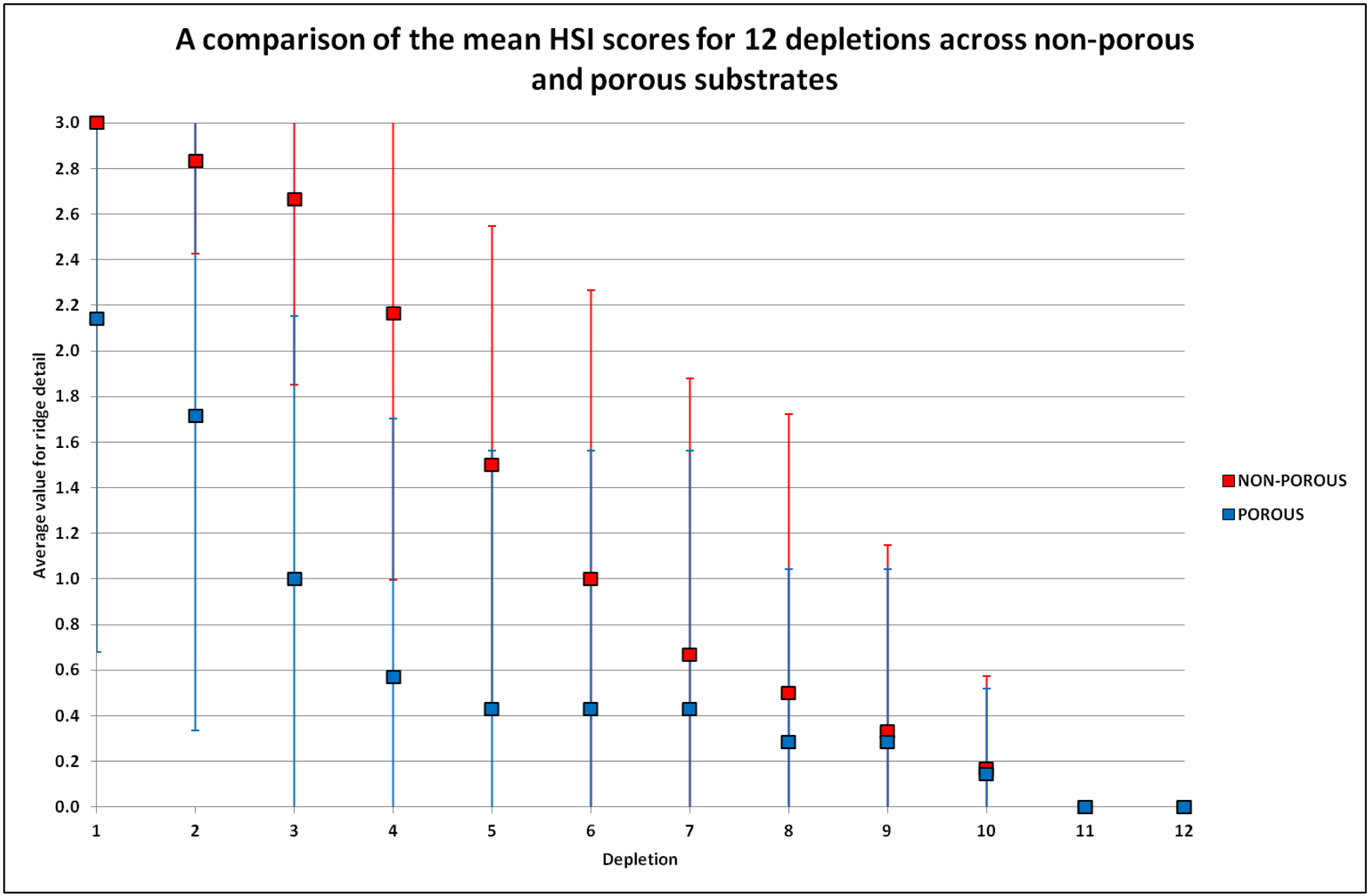
A comparison of the mean HSI scores for 12 depletions across non-porous and porous substrates
Average value for ridge detail
3.0
2.8
2.6
2.4
2.2
2.0
1.8
1.6
1.4
1.2
1.0
0.8
0.6
0.4
0.2
0.0
1
2
3
4
5
6
7
8
9
10
11
12
Depletion
NON-POROUS
POROUS

Figure 10

WET/DRY	DILUTION	DSLR	HSI
WET	PURE		
	10 FOLD	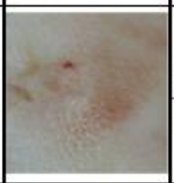	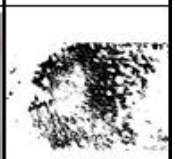
	100 FOLD		
	1000 FOLD		
	1500 FOLD		
DRY	PURE		
	10 FOLD		
	100 FOLD		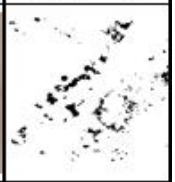
	1000 FOLD		
	1500 FOLD